Gaze Scanning at Street Crossings by Pedestrians With Homonymous Hemianopia With and Without Hemispatial Neglect

Shrinivas Pundlik,[1] Matteo Tomasi,[1,*] Kevin E. Houston,[1,2] Ayush Kumar,[1] Prerana Shivshanker,[1] Alex R. Bowers,[1] Eli Peli,[1] and Gang Luo[1]

[1]Schepens Eye Research Institute of Mass Eye & Ear, Harvard Medical School Department of Ophthalmology, Boston, Massachusetts, United States
[2]University of Massachusetts Chan Medical School, Central Western Massachusetts Veterans Affairs, Massachusetts, United States

Correspondence: Shrinivas Pundlik, Harvard Medical School, Schepens Eye Research Institute of Mass Eye & Ear, 20 Staniford St., Boston, MA 02114, USA; shrinivas_pundlik@meei.harvard.edu.

Current Affiliation: *EyeNexo LLC, Boston, Massachusetts, United States.

Received: May 16, 2023
Accepted: October 19, 2023
Published: November 17, 2023

Citation: Pundlik S, Tomasi M, Houston KE, et al. Gaze scanning at street crossings by pedestrians with homonymous hemianopia with and without hemispatial neglect. *Invest Ophthalmol Vis Sci.* 2023;64(14):26. https://doi.org/10.1167/iovs.64.14.26

Purpose. To investigate compensatory gaze-scanning behaviors during street crossings by pedestrians with homonymous hemianopia (HH) and hemispatial neglect (HSN).

Methods. Pedestrians with right homonymous hemianopia (RHH) and left homonymous hemianopia without (LHH) and with left spatial-neglect (LHSN) walked on city streets wearing a gaze-tracking system that also captured scene videos. Street-crossing instances were manually annotated, and horizontal gaze scan of magnitude $\geq$20° and scanning rates were compared within-subject, between the side of the hemifield loss (BlindSide) and the other side (SeeingSide). Proportion of instances with scans to both the left and the right side at nonsignalized crossings (indicative of safe scanning behavior) were compared among the three subject groups.

Results. Data from 19 participants (6 LHH, 7 RHH, and 6 with mild [4] or moderate [2] LHSN), consisting of 521 street-crossing instances of a total duration of 201 minutes and 5375 gaze scans, were analyzed. The overall gaze magnitude (mean [95% confidence interval (CI)]) was significantly larger toward the BlindSide (40.4° [39.1°–41.9°]) than the SeeingSide (36° [34.8°–37.3°]; $P < 0.001$). The scanning rate (mean [95% CI] scans/min) toward the BlindSide (14 [12.5–15.6]) was significantly higher than the SeeingSide (11.5 [10.3°–12.9°]; $P < 0.001$). The scanning rate in the LHSN group (10.7 [8.9–12.8]) was significantly lower than the LHH group (14 [11.6–17.0]; $P = 0.045$). The proportion of nonsignalized crossings with scans to both sides was significantly lower in LHSN (58%; $P = 0.039$) and RHH (51%; $P = 0.003$) than LHH (75%) participants.

Conclusions. All groups demonstrated compensatory scanning, making more gaze scans with larger magnitudes to the blind side. Mild to moderate LHSN adversely impacted the scanning rate.

Keywords: hemispatial neglect, naturalistic mobility, visual field loss, mobile gaze, homonymous hemianopia, stroke, brain injury

Homonymous hemianopia (HH), the loss of one-half of the visual field on the same side in both eyes, is associated with mobility-related challenges, such as impaired hazard detection and collisions with obstacles.[1–4] Individuals with HH may perform compensatory gaze movements toward (or into) their blind field.[5–12] However, little is known about gaze-scanning behaviors of pedestrians with HH at street crossings as most previous studies have been in the context of driving.[8,10–13] At intersections, driving simulator studies have found that head- and gaze-scanning behavior of drivers with HH is predictive of safe detection of peripheral hazards approaching along the cross streets.[13,14]

The gaze behavior of pedestrians has been studied in the context of traffic safety to investigate the effects of age, attention, or vision loss on street-crossing performance.[15] Previous studies of street-crossing behavior in visually impaired pedestrians focused on a variety of aspects: scene elements where pedestrians fixate their gaze,[16] gross categorization of head scan direction (categorized as left, center, or right),[17] traffic gap detection,[18–20] judgment of crossing time,[21] and overall decision-making.[22–24] While these studies included a mix of normal-vision controls and people with central and peripheral vision loss, none addressed people with HH, and the one study that evaluated head movements at pedestrian street crossings did not use quantitative head-tracking data.[17]

This paucity of evidence regarding pedestrian gaze scanning extends to patients with HH with a history of hemispatial neglect (HSN). Neglect commonly occurs with left HH and frequently results in reduced gaze shifts toward the left.[25] Patients with HSN are less likely to have insight of their deficits (anosognosia),[26,27] including their visual field loss, decreasing the likelihood that a compensatory scanning behavior would be employed at intersections or otherwise. If

they do scan, the magnitude may be insufficient because of directional hypokinesia, where movements to the left versus right are of reduced amplitude and velocity (a component of motor-intentional neglect[28]).

Recording mobile gaze data in unrestricted outdoor environments is challenging and is one of the reasons for the paucity of evidence about naturalistic gaze-scanning behaviors when walking. Using methods and protocols for the collection and processing of noisy outdoor gaze data,[29,30] we present a quantitative analysis of gaze scanning at pedestrian street crossings during natural walking of individuals with either left homonymous hemianopia (LHH), right homonymous hemianopia (RHH), or mild to moderate left hemispatial neglect (LHSN). We investigated the within-subject compensatory scanning behaviors toward the blind hemifield and whether individuals with LHSN exhibited gaze-scanning deficits compared to those without HSN. Our expectation was that study results may guide rehabilitation efforts such as compensatory scanning training[6,31–33] or mobility aid development.[34–37]

Methods

The data analyzed in this article were originally acquired between 2012 and 2014 in two studies involving individuals with HH and LHSN that used the same experimental procedures (Appendix A).[5,38,39] The data were collected over multiple visits (up to four). The study protocols were approved by the Institutional Review Board at Mass Eye & Ear and the US Army Medical Research and Material Command (USAMRMC), Human Research Protection Office (HRPO). The studies followed the tenets of the Declaration of Helsinki, and written informed consent was obtained from all the participants. The collected data could be made available for research purposes upon request.

Participants

Participants were recruited from optometry, ophthalmology, and rehabilitation medicine practices within the Greater Boston area and from a billing database search at Massachusetts Eye and Ear Infirmary for patients with a diagnosis of HH field defect (Appendix A). Inclusion criteria were as follows: HH with or without hemispatial neglect, at least 14 years of age, >3 months since vision loss (caused by cerebrovascular event), visual acuity 20/50 or better in each eye, ability to walk independently without assistance from a sighted guide, and no severe vertigo or vestibular dysfunction. Screening for eligibility included a case history, distance visual acuity, Goldmann visual fields (V4e target), and hemineglect screening with the Schenkenberg line bisection test,[40] Bells cancellation test,[41] and the Catherine Bergego Scale.[42] Cognitive status was quantified with either the Montreal Cognitive Assessment test or Mini-Mental Status Exam (MMSE).[43] Patients with LHSN were diagnosed by a vision rehabilitation specialist (author KEH) on the basis of formal screening tests, subjective history, review of medical records, and lesion location. A total of 22 participants were enrolled of which 3 were excluded from analyses (1 RHH did not cross any streets, 1 LHSN used a motorized scooter, and 1 LHH with no recorded head movement data).

Study Procedures

During each visit, participants walked one of two predetermined routes, along the sidewalks on the opposite sides

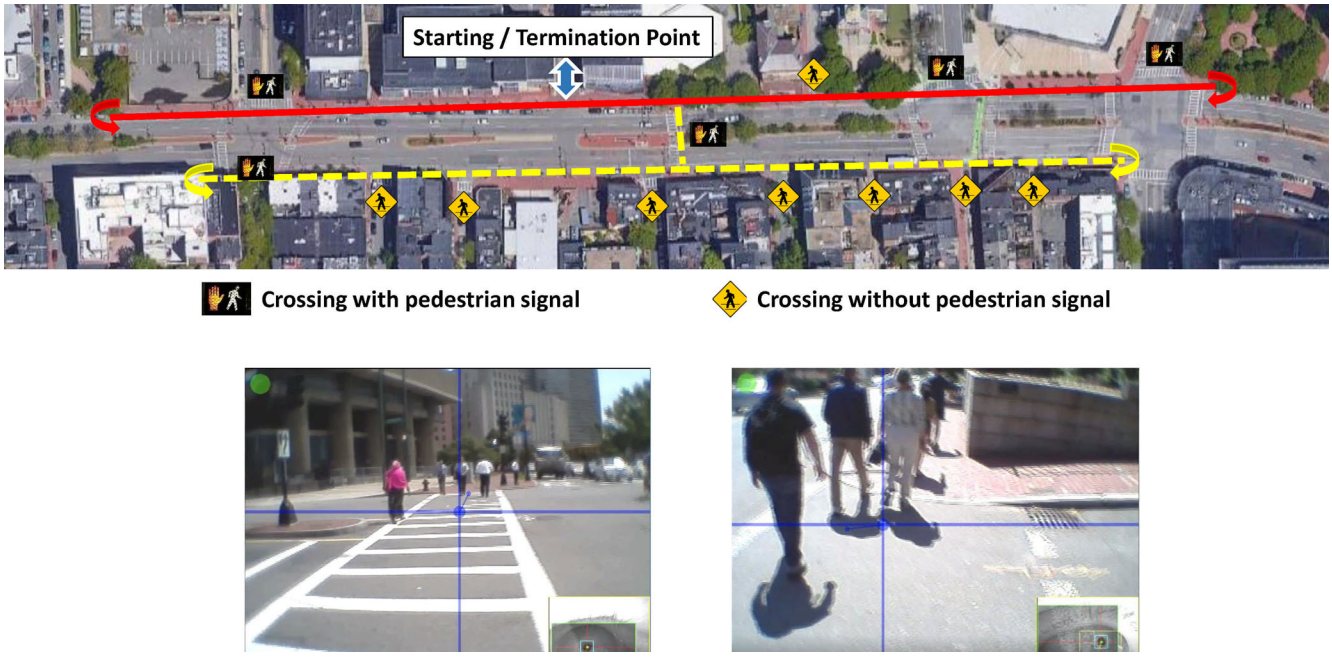

Figure 1. *Top*: Outdoor walking routes. A satellite image from Google Maps overlaid with the two walking routes (*solid red line* and *dashed yellow line*) on the opposite sides of a stretch of Cambridge Street in Boston, Massachusetts. All walks started and ended at the same point indicated in the figure. To get to the route on the opposite side of the road (*dashed yellow line*), the participants crossed the street at a signalized crossing (*yellow dashed line* overlaid on the street). In each route, the participants turned around and traversed the same path in the opposite direction (indicated by U-shaped *arrows* at the ends of each line). At the U-turn at each end of the route, the heading direction of the inertial sensors was reset. Each route involved a different combination of street crossings with and without pedestrian signals. *Bottom*: Screenshots of signalized (*left*) and nonsignalized (*right*) crossings from the scene camera. The *blue crosshairs* indicate the eye-in-head position mapped on the scene camera image for visualization.

Investigative Ophthalmology & Visual Science

of a busy street in downtown Boston (Fig. 1). All walks were performed during the daytime. Each route was approximately straight with a U-turn on each end. The participant traversed each route in both directions (round trip distance ≈0.6 miles). In total, there were 10 street crossings with pedestrian signals (5 locations × 2 walking directions) and 16 nonsignalized crossings (8 locations × 2 walking directions). Fourteen crossings had two-way traffic, and 12 had one-way traffic (6 each from the left and right).

The participants wore a custom-developed mobile gaze recording setup that consisted of a commercial mobile eye tracker with a scene camera (Positive Science, New York, NY, USA), measuring eye-in-head movement, and a head-tracking system based on two inertial sensors (VectorNav, Dallas, TX, USA). Details of the gaze-tracking system and its evaluation were previously described.[29] The system was connected to laptops in a backpack worn by the pedestrian, where the scene videos and eye and head movement data were logged for offline processing.

The eye-tracking setup allowed the participants to wear their habitual refractive correction while walking. Participants were instructed to walk as they normally would, to cross streets as they normally would with due regard for safety, and to use pedestrian crossing signals when available. They were not given any specific instructions about scanning, although they were aware that their head and eye movements were being recorded. A researcher walked behind the participant to ensure participant safety.

Gaze Computation

Gaze shift is a combination of head and eye-in-head movements, which were independently obtained by our gaze-tracking system. The eye movement measurements were converted to angular values and synchronized with the head movements.[29] The head-tracking unit consisted of one head-mounted inertial sensor and another mounted on the waist-belt. Each sensor output had orientation signals in terms of yaw, pitch, and roll angles. A differential signal was derived from the dual-inertial sensor design, which provided a measure of head orientation with respect to the body trunk (the medial position/heading direction) and also helped mitigate the signal drift due to correlated external interferences (e.g., electromagnetic signals) present in outdoor urban environments.

The differential head orientation data from the inertial sensors could still be intermittently affected by noise. Therefore, head movements were also estimated on the basis of the imagery captured by the scene camera, independent of the inertial sensors, via the methodology of monocular Simultaneous Localization and Mapping (SLAM).[30] SLAM provided more accurate head movement estimates but was prone to intermittent tracking failures, resulting in data loss. The signals from the inertial sensors, on the other hand, were continuously available, albeit noisy. The head movements obtained via SLAM were fused with those obtained with the inertial sensors (see Appendix B) to obtain a more reliable head movement signal. The eye movements were combined with the synchronized fused head movement signal to obtain gaze positions for each video frame (≈30 samples/s).

Gaze Scans at Street Crossings

Horizontal gaze scans >20° on either side with respect to the mean heading direction were identified from the gaze data (Appendix C). The 20° threshold helped retain scans that were relevant for scanning at crossings. In previous driving simulator studies,[13,44] scans ≥20° when approaching an intersection were found to be highly predictive of successful detection of peripheral hazards.

Street-crossing instances were manually identified and marked from the associated scene videos, and gaze scans were analyzed for the identified segments. The type of crossing (with or without pedestrian signal) was recorded. Additionally, two phases were identified for each crossing segment: (1) approach—starting from when the participant passed the walk signal button or the signpost with the cross-street name until stepping into the street (this phase also included wait time) and (2) crossing—starting from when the participant stepped into the street until stepping on the sidewalk at the other side. The scanning side with respect to the body midline (which was aligned with the walking direction) was also annotated, that is, whether the scan was toward the blind hemifield (BlindSide) or toward the side where vision was intact (SeeingSide).

Outcomes

The two main outcome measures of scanning performance were gaze scan magnitude (in degrees, measured with respect to the straight-ahead heading direction) and the scanning rate (number of scans per minute). Gaze data loss affected the computation of scanning rate. There was greater loss of the eye movements compared to the head. Consequently, the gaze data loss was always greater than or equal to the head movement data loss. Therefore, when the gaze scan peak was missing but the corresponding head scan magnitude was ≥20°, it was also included as a scan (such cases were <2% of all scans), in addition to all available gaze scans ≥20°. The number of scans was aggregated at the level of each crossing instance and normalized to a scanning rate by the time duration of head movement data availability (which was always larger than or equal to the corresponding gaze data availability). For analysis of gaze magnitude, all available gaze scans with magnitude ≥20° were considered. Additionally, we compared the between-group differences in the proportion of nonsignalized crossing instances where the participants looked both ways before crossing the street, thereby exhibiting safe crossing behavior.

Statistical Analysis

Multilevel mixed-effects regression models were used to determine the association between scanning behavior outcomes and key predictors/fixed effect factors: scanning side (side of hemifield loss: BlindSide or SeeingSide), patient group (LHH, RHH, or LHSN), type of crossing (signalized or nonsignalized), crossing phase (approach versus crossing), age, and years since onset. MMSE score was found to be collinear with subject group and therefore not included in the analysis. Visit nested within subjects was modeled as random intercepts.

Linear mixed-effects regression was used for scanning magnitude (reciprocal inverse log transformed for better fit). For scanning rate, the number of scans was modeled as overdispersed count data in a mixed-effects negative binomial model.[34,45] The proportion of safe crossing instances (scans to both right and left sides) was compared among the three groups using the χ^2 test of proportionality.

Estimated marginal means (back-transformed) with their 95% confidence intervals (CIs) and contrasts obtained from the linear regression model for scanning magnitude are

reported. Incidence rate ratios are reported from the count regression model for the scanning rate. P values <0.05 were considered statistically significant. Statistical analysis was performed using statistical packages in R (ver. 4.0.4; R Foundation for Statistical Computing, Vienna, Austria).[46–51] The details of the statistical analysis, including the packages used, model specifications, and evaluation, are presented in Appendix D.

Results

Data from 19 participants were included in the analyses: 6 with LHH, 6 with mild to moderate LHSN, and 7 with RHH (see Table 1 for summary statistics and Appendix A for subject-level details). All LHSN participants in our study also had LHH. Out of the 19 participants, 16 had complete hemianopia, 2 had macular sparing (of 5° to 10°), and 1 had some residual vision in the far peripheral field on the blind side beyond about 60° eccentricity horizontally and 50° inferiorly. Testing was not performed to evaluate statistical significance for groupwise differences in participant characteristics since sample sizes were small in each group; however, each of these factors (age, gender, and years since onset) was evaluated as a potential predictor of scanning rate and gaze magnitude in univariate analyses. A total of 549 crossing instances were annotated from all the recorded data. For the analysis of scanning rate, 28 crossing instances were dropped due to data loss. Available data in the remaining 521 crossing instances spanned a total of 201 minutes and yielded 5481 scans. Only 2% had missing gaze peak magnitude (were head-only scans). In total, 5375 gaze scans were available for the analysis of gaze magnitude. The head position was concordant with gaze 90% of the time (head angle with same sign as gaze). Forty-nine percent of gaze scans involved a large head contribution of >10° magnitude (mean ± SD overall gaze magnitude: 55° ± 23°).The rest of the gaze scans (51%) comprised mainly eye movements with little or no head movement and tended to be smaller in magnitude (36° ± 14°) than gaze scans with a larger head movement contribution.

Compared to the SeeingSide, there were more scans ≥40° toward the BlindSide (Fig. 2A; Table 2), with significantly larger average gaze magnitude (mean [95% CI]; SeeingSide: 36° [34.8°–37.3°], BlindSide: 40.4° [39.1°–41.9°]; $P < 0.001$). For all three subject groups, the gaze magnitude was significantly larger toward the BlindSide than the SeeingSide (Fig. 2B) and during the approach phase than the crossing phase (Fig. 2C). The gaze magnitude was significantly larger toward the BlindSide than the SeeingSide in all three groups during the approach phase and in LHH and RHH groups during the crossing phase. No significant difference in the gaze magnitude between the two sides was seen during the crossing phase in the LHSN group (Fig. 2D). Gaze magnitude was larger at nonsignalized crossings than signalized crossings in the LHSN group (Fig. 2E).

Scanning rate was significantly higher, by about 21%, toward the BlindSide than the SeeingSide (mean [95% CI] scans/min; SeeingSide: 11.5 [10.3°–12.9°], BlindSide: 14 [12.5°–15.6°]; $P < 0.001$) and significantly lower during the crossing phase, by about 38%, compared to the approach phase (mean scans/min [95% CI]; approach: 15.3 [13.7–17.1], crossing: 10.6 [9.44–11.8]; $P < 0.001$) (Table 3). Scanning rate declined by about 1% per decade advance in age. Overall scanning rate of LHSN participants was significantly lower, by about 24%, than LHH participants (mean [95% CI] scans/min; LHH: 14 [11.6–17.0], LHSN: 10.7 [8.9–12.8]; $P = 0.045$). There was a significant interaction between the crossing phase and crossing type factors, as the difference between the scan rate during the approach and crossing phases was larger at nonsignalized crossings than at signalized crossings (approach-crossing; NoSignal: 6.1 scans/min, Signal: 3.31 scans/min; $P = 0.007$).

The LHSN and RHH participants failed to look both ways at a higher proportion of nonsignalized crossing instances compared to the LHH participants, despite the LHH group experiencing significantly higher data loss compared to the LHSN and RHH groups (Table 4). The LHH group looked both ways at 72 out of 96 nonsignalized crossings (75%), whereas the LHSN and RHH groups only looked both ways at 57 out of 98 (58%) and 45 out of 89 crossings (51%), respectively. The proportion of one-way streets and the direction of traffic encountered by the three groups was not significantly different. There was no significant difference in the proportion of crossing instances with both-way scans among the three directions of the cross traffic. The participants were significantly more likely to scan both ways at a crossing if the main street (parallel to the walking direction) happened to be on the blind side (71% of instances with both-side scans) than their seeing side (51% of instances

Table 1. Participant Characteristics and Descriptive Overview of Street-Crossing Data

Characteristic	Overall	LHH	LHSN	RHH
N	19	6	6	7
Age, median [25th–75th percentile]	53 [46–73]	50 [46–59]	50 [39–66]	63 [53–73]
Males, *n* (%)	14 (74)	3 (50)	6 (100)	5 (71)
Years since onset,* median [25th–75th percentile]	2.4 [1.2–4.2]	3.0 [2.2–3.9]	3.5 [1.7–12.8]	1.3 [0.8–1.8]
MMSE scores,† median [25th–75th percentile]	28 [25.5–29]	29 [29–29.75]	26.5 [25.25–27]	27 [24–28.5]
Head movement data loss, median [25th–75th percentile], %	3.7 [0–16]	3.4 [0–17]	3.7 [0–15]	4.0 [0–16]
No. of street crossings	521	161	187	173
With pedestrian signal	238	65	89	84
Without pedestrian signal	283	96	98	89
Duration in minutes (avail. data)	201	61	70	68
Approaching	117	29	42	46
Crossing	84	21	30	32
No. of gaze scans (gaze magnitude analysis)	5375	1510	1596	2269
SeeingSide	2470	657	758	1055
BlindSide	2905	853	838	1214

* Data missing for one patient with LHH.
† Scores for two participants converted from the Montreal Cognitive Assessment based on the conversion table in Kim et al.[52]

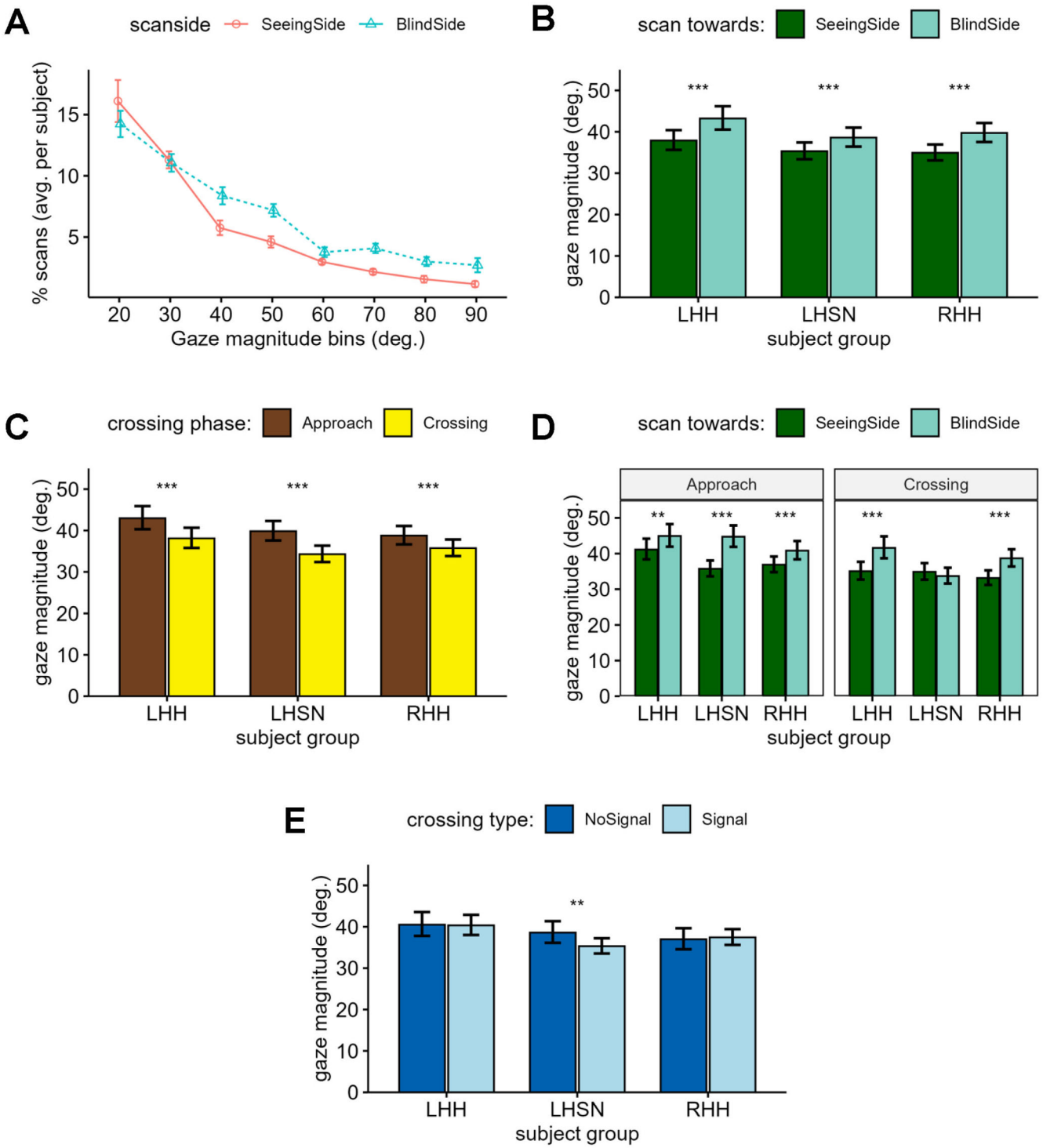

Figure 2. Analysis of gaze magnitude at street crossings. (**A**) Distribution of the average percentage of gaze scans for BlindSide versus SeeingSide over different gaze magnitudes. The *error bars* show the standard error of the mean computed over 19 participants. The average percentage of large scans (magnitude ≥40°) was higher toward the BlindSide. (**B–E**) Estimated marginal mean gaze magnitude, with *error bars* showing the 95% confidence interval of mean. (**B**) Gaze magnitude was significantly larger toward the BlindSide than SeeingSide for all three subject groups. (**C**) Gaze magnitude was larger in the approach phase than the crossing phase in all three subject groups. (**D**) Significant interaction between subject group, crossing phase, and scanning side, primarily because the difference between BlindSide and SeeingSide gaze magnitudes was not significant in the crossing phase for the LHSN group. (**E**) Significantly higher gaze magnitude in nonsignalized than signalized crossings, only for the LHSN group. Significance levels: ***$P < 0.001$, **$P = 0.001$–0.01, and *$P = 0.01$–0.05.

Investigative Ophthalmology & Visual Science

Table 2. Estimated Marginal Means and Their 95% CIs From the Linear Regression Model Analyzing Gaze Magnitude

Characteristic	Estimated Mean Gaze Magnitude [95% CI], deg		*P* Value
	Factor Level 1	Factor Level 2	
Scanning side	SeeingSide	BlindSide	
Group—LHH	37.9 [35.6–40.4]	43.2 [40.5–46.2]	<0.001
Group—LHSN	35.3 [33.4–37.4]	38.6 [36.4–41.0]	<0.001
Group—RHH	34.9 [33.1–36.9]	39.7 [37.5–42.1]	<0.001
Crossing phase	Approach	Crossing	
Group—LHH	43.0 [40.3–45.9]	38.1 [35.8–40.7]	<0.001
Group—LHSN	39.8 [37.6–42.3]	34.3 [32.4–36.3]	<0.001
Group—RHH	38.8 [36.6–41.1]	35.7 [33.8–37.8]	<0.001
Crossing type	NoSignal	Signal	
Group—LHH	40.5 [37.8–43.6]	40.3 [38.0–42.9]	1.0
Group—LHSN	38.6 [36.1–41.3]	35.3 [33.5–37.2]	0.002
Group—RHH	37.0 [34.6–39.7]	37.4 [35.6–39.4]	1
Scanning side by crossing phase			
Approach	SeeingSide	BlindSide	
Group—LHH	41.1 [38.4–44.2]	44.9 [41.9–48.3]	0.004
Group—LHSN	35.7 [33.6–38.1]	44.7 [41.9–47.9]	<0.001
Group—RHH	36.9 [34.8–39.2]	40.8 [38.4–43.5]	<0.001
Crossing			
Group—LHH	35.1 [32.7–37.7]	41.6 [38.7–44.8]	<0.001
Group—LHSN	34.9 [32.7–37.3]	33.7 [31.6–36.0]	0.29
Group—RHH	33.1 [31.2–35.3]	38.7 [36.4–41.2]	<0.001

P value adjustment method for multiple pairwise comparison: Holm.

Table 3. Incidence Rate Ratios and Their 95% CIs From the Regression Model Analyzing Scanning Rate

Predictor [Unit/Category Level]	Incidence Rate Ratio	95% CI	*P* Value
Age [in decade]	0.990	0.984–0.996	**0.001**
Scanning side [BlindSide]	1.210	1.126–1.300	**<0.001**
Group [LHSN]	0.765	0.590–0.994	**0.045**
Group [RHH]	0.977	0.758–1.261	0.860
Crossing phase [Crossing]	0.620	0.542–0.709	**<0.001**
Crossing type [Signal]	0.905	0.804–1.018	0.096
Crossing phase [Crossing] × crossing type [Signal]	1.245	1.061–1.461	**0.007**

The reference levels when computing rate ratios for categorical predictors were as follows: (1) scanning side: SeeingSide, (2) group: LHH, (3) crossing phase: approach, and (4) crossing type: NoSignal.

with both-side scans). However, since there were two walking routes on each side of the road and since the participants walked each route in both directions, the crossing instances with the main road toward the blind side and seeing side were closely balanced across the three subject groups.

Discussion

We analyzed the gaze-scanning behaviors of individuals with homonymous hemianopia and hemispatial neglect while crossing busy urban streets, thereby providing first-of-its-kind, real-world data in this cohort of individuals during this important task. The average BlindSide scanning rate was higher by 22% (a 2.5-scan/min difference) than toward the SeeingSide, and the gaze magnitude was slightly larger by 12% (about 4.4°) toward the BlindSide compared to the SeeingSide. These findings suggest that participants were using compensatory scanning behaviors (more and larger scans to the BlindSide) to address the hemifield loss. However, individuals with LHSN scanned significantly less often overall, by about 3.3 scans/min, than LHH. They also showed a relatively lower propensity to scan toward both sides at nonsignalized crossings than the LHH group. These differences may be indicative of the possible impact of HSN on scanning behavior at street crossings.

The finding that HH pedestrians scanned more frequently toward their BlindSide than their SeeingSide is consistent with our preliminary findings (street crossings not analyzed

Table 4. GroupWise Breakdown of Gaze Data Loss and Scanning Toward Both Sides at Nonsignalized Crossings

Characteristic	GroupWise, %			*P* Values for Pairwise Comparisons		
	LHH	LHSN	RHH	LHH vs. LHSN	LHH vs. RHH	LHSN vs. RHH
Instances with a scan to both left and right sides	75	58	51	0.039	0.003	0.37
Gaze data loss	37	33	37	<0.001	0.75	<0.001

P-adjustment method: Holm.

separately) from a small subset of participants from this outdoor walking study[5] and with driving studies of scanning at intersections.[8,12] Drivers with HH who were rated as safe in a road test made more head scans to their BlindSide than those who were rated as unsafe.[12] While we found a small (≈4°) but statistically significant increase in gaze magnitude toward the BlindSide, findings in previous studies were mixed. A driving simulator–based study of HH drivers by Papageorgiou et al.[11] showed significantly larger gaze amplitude toward the seeing side compared to the blind side. On the other hand, Xu et al.[53] showed HH drivers scanned with significantly larger gaze magnitudes toward the blind side. A few previous studies only analyzed head scans in drivers with HH. There was no significant difference in the head scan magnitude toward the seeing side and the blind side in the study by Bowers et al.[8] An on-road driving study by Wood et al.[12] reported more large and small head scans toward the blind side in a subset of participants with HH who were deemed safe drivers but not in the unsafe drivers, but the magnitude was not measured. However, this effect size was the average over a large range of gaze magnitudes. For scans with magnitude <40°, the relative proportion of scans to the blind and seeing sides did not differ (Fig. 2A). In contrast, for scans with magnitude ≥40°, there was a consistently higher proportion of scans toward the blind than the seeing side. Thus, even as the average gaze magnitude difference between the levels of a factor may be small (e.g., difference between BlindSide and SeeingSide), the relative frequency of scans over different gaze magnitudes could provide further insights into the gaze behavior in different conditions.

Overall reduced scanning rate and smaller gaze magnitudes *during* the crossing phase compared to when the pedestrians approached the street crossing seem reasonable given that scanning for traffic should be done primarily before starting to cross. Similar behaviors were reported in previous studies of visually impaired pedestrians, in which there was a more central head position and fixation on traffic elements such as crosswalks or traffic lights during the crossing phase.[16,17] We also found that the effect of the crossing phase on gaze magnitude toward the BlindSide versus SeeingSide differed in the three groups. LHSN participants scanned toward their BlindSide with significantly larger gaze magnitudes during the approach phase but not during the crossing phase (Fig. 2D). On the other hand, LHH and RHH participants scanned toward their BlindSide with significantly larger gaze magnitudes regardless of the crossing phase. This may be another indication of the impact of hemispatial neglect in the LHSN group: when their covert attention was on the forward crossing task, attention to the far periphery was diminished. While difficulties in dividing attention could mean that individuals with HSN could not perform compensatory scanning when focusing on crossing the street, there could be other contributing factors for the observed differences between LHH and LHSN groups. There could be issues related to the neglect such as balance impairment, which means they have to concentrate more on walking, or problems with awareness (anosognosia), which could lead to impaired judgment of potential hazards. Evaluation of these factors was beyond the scope of this study but could be considered in future studies.

We did not find any significant difference in the overall scanning rate between signalized and nonsignalized crossings. This result is consistent with the finding by Hassan et al.[17] of no significant difference in scanning rates between plus (signalized) and roundabout (nonsignalized) crossings. However in our study, the type of crossing (signalized versus nonsignalized) affected one group of participants—people with LHSN had significantly larger gaze magnitude at nonsignalized crossings than signalized crossings (Fig. 2E).

There was a significant interaction between crossing type and crossing phase for scan rate (Table 3), as the difference in the scanning rate between the approach and crossing phases was larger at nonsignalized crossings than at signalized crossings. One possible reason for this effect could be because at signalized crossings, the signal lights indicate when it should be safe to cross and therefore the scanning rate was slightly reduced during the approach phase at signalized crossings compared to the same at nonsignalized crossings (but the difference was not statistically significant).

We had expected that the individuals with LHSN would show a larger deficit in their scanning to their neglected side due to the characteristically reduced awareness for the deficit, impaired leftward spatial attention, and leftward hypokinesia,[25] but this sample of individuals with mild to moderate LHSN appeared to be just slightly more impaired than the LHH group in their gaze-scanning behaviors. Relative to the LHH group, LHSN participants as a group scanned less frequently (Table 3) and scanned both ways less frequently at nonsignalized crossings (Table 4), and the BlindSide versus SeeingSide difference in the scan magnitude was not significant during the crossing phase—contrary to the trends in the other two subject groups. However, caution should be used in trying to generalize this finding to the clinical LHSN populations. Our sample was small and the LHSN individuals were independently ambulatory (inclusion required that they were able to walk without assistance) and as a result had only mild to moderate LHSN. A sample with severe cases would likely have greater scanning deficits.

Analysis of scanning at nonsignalized crossings may provide insights into the safety of the scanning behaviors of the pedestrians with HH. Generally, scanning to both left and right sides is considered a good practice, regardless of the cross-traffic direction, especially at nonsignalized crossings. But in our study, we found absence of two-way scanning in multiple nonsignalized crossing instances (Table 4). Both LHSN and RHH participants were significantly less likely to scan in both directions than the LHH participants, suggesting that the LHSN and RHH participants had less safe scanning behaviors. One could argue that scans might have been made but were missed due to the data losses, which could account for the between-group differences. However, the difference in data loss (Table 4) among the three groups was small (despite the *P* values, which are because of very large samples). Compared to the small differences in the data loss, there was a large difference in the proportion of instances with two-way scans, indicating a valid effect. Furthermore, based on our analysis, it is unlikely that the difference between LHH and the rest was related to the side of the road (main street) or the direction of traffic at the crossings.

Our finding that scanning rate declined with age was consistent with previous findings in the context of driving.[54,55] While our study sample had more males than female, gender was not associated with scanning rate or gaze magnitude. Previous studies had reported that even though men engaged in somewhat riskier crossing behavior than females, the differences in gaze patterns were mostly observed in terms of where each group looked in their surrounding before or during crossing streets.[56,57]

Investigative Ophthalmology & Visual Science

There are several limitations to our analysis. Data for normally sighted participants were lacking since the original data collection was done under a development and pilot study and did not include recruitment of a control group due to funding agency stipulation. Also, while data were rich with many repeated measures over multiple visits, the patient sample in each group was relatively small, which potentially reduced the power of the between-group findings. Despite these limitations, this is the first study to successfully measure within-subject compensatory gaze scanning at street crossings in people with HH and HSN. Understanding scanning behavior could inform rehabilitation practices. Compensatory scanning training may be beneficial for mobility of patients with visual field loss. Our data suggest that compensatory scanning has already developed to some extent in our study population. Scanning training may be more helpful for individuals who had recent onset of brain injury with field loss. Further, scanning training should focus on head movement in street crossing, because the magnitude of scans for safe crossing might not be achievable with eye movements alone. In addition to the training of compensatory scanning to the blind side, scanning to both sides before crossing, especially at nonsignalized crossings, may need to be emphasized.

Acknowledgments

Supported by National Institutes of Health grant EY031444. The original data collection study was supported by Department of Defense grant DM090420.

Disclosure: **S. Pundlik**, None; **M. Tomasi**, None; **K.E. Houston**, None; **A. Kumar**, None; **P. Shivshanker**, None; **A.R. Bowers**, None; **E. Peli**, None; **G. Luo**, None

References

1. de Haan GA, Heutink J, Melis-Dankers BJ, Brouwer WH, Tucha O. Difficulties in daily life reported by patients with homonymous visual field defects. *J Neuroophthalmol*. 2015;35:259–264.
2. Jones S, Shinton R. Improving outcome in stroke patients with visual problems. *Age Ageing*. 2006;25:560–565.
3. Bowers AR, Mandel AJ, Goldstein RB, Peli E. Driving with hemianopia, I: detection performance in a driving simulator. *Invest Ophthalmol Vis Sci*. 2009;50:5137–5147.
4. Alberti CF, Peli E, Bowers AR. Driving with hemianopia, III: detection of stationary and approaching pedestrians in a simulator. *Invest Ophthalmol Vis Sci*. 2014;55:368–374.
5. Tomasi M, Bowers AR, Peli E, Luo G. Compensatory gaze scanning by patients with hemianopia during outdoor walking. *Invest Ophthalmol Vis Sci*. 2014;55:4131.
6. de Haan GA, Melis-Dankers BJM, Brouwer WH, Tucha O, Heutink J. The effects of compensatory scanning training on mobility in patients with homonymous visual field defects: a randomized controlled trial. *PLoS ONE*. 2015;10:e0134459.
7. Pambakian ALM, Kennard C. Can visual function be restored in patients with homonymous hemianopia? *Br J Ophthalmol*. 1997;81:324–328.
8. Bowers AR, Ananyev E, Mandel AJ, Goldstein RB, Peli E. Driving with hemianopia, IV: head scanning and detection at intersections in a simulator. *Invest Ophthalmol Vis Sci*. 2014;55:1540–1548.
9. Bahnemann M, Hamel J, De Beukelaer S, et al. Compensatory eye and head movements of patients with homonymous hemianopia in the naturalistic setting of a driving simulation. *J Neurol*. 2015;262:316–325.
10. Kübler T, Kasneci E, Rosenstiel W, et al. Driving with homonymous visual field defects: driving performance and compensatory gaze movements. *J Eye Mov Res*. 2015;8:1–11.
11. Papageorgiou E, Hardiess G, Mallot H, Schiefer U. Gaze patterns predicting successful collision avoidance in patients with homonymous visual field defects. *Vis Res*. 2012;65:25–37.
12. Wood JM, McGwin G, Jr, Elgin J, et al. Hemianopic and quadrantanopic field loss, eye and head movements, and driving. *Invest Ophthalmol Vis Sci*. 2011;52:1220–1225.
13. Swan G, Savage SW, Zhang L, Bowers AR. Driving with hemianopia, VII: predicting hazard detection with gaze and head scan magnitude. *Transl Vis Sci Technol*. 2021;10:20.
14. Hardiess G, Hansmann-Roth S, Mallot H. Gaze movements and spatial working memory in collision avoidance: a traffic intersection task. *Front Behav Neurosci*. 2013;7:1–13.
15. Lévêque L, Ranchet M, Deniel J, Bornard JC, Bellet T. Where do pedestrians look when crossing? A state of the art of the eye-tracking studies. *IEEE Access*. 2020;8:164833–164843.
16. Geruschat DR, Hassan SE, Turano KA, Quigley HA, Congdon NG. Gaze behavior of the visually impaired during street crossing. *Optom Vis Sci*. 2006;83:550–558.
17. Hassan SE, Geruschat DR, Turano KA. Head movements while crossing streets: effect of vision impairment. *Optom Vis Sci*. 2005;82:18–26.
18. Cheong AM, Geruschat DR, Congdon NG. Traffic gap judgment in people with significant peripheral field loss. *Optom Vis Sci*. 2008;85:26–36.
19. Geruschat DR, Fujiwara K, Wall Emerson RS. Traffic gap detection for pedestrians with low vision. *Optom Vis Sci*. 2011;88:208–216.
20. Hassan SE. Are normally sighted, visually impaired, and blind pedestrians accurate and reliable at making street crossing decisions? *Invest Ophthalmol Vis Sci*. 2012;53:2593–2600.
21. Graber M, Hassan S. The mind cannot go blind: effects of central vision loss on judging one's crossing time. *Optom Vis Sci*. 2020;97:406–415.
22. Almutleb ES, Hassan SE. The effect of simulated central field loss on street-crossing decision-making in young adult pedestrians. *Optom Vis Sci*. 2020;97:229–238.
23. Hassan SE, Massof RW. Measurements of street-crossing decision-making in pedestrians with low vision. *Accident Anal Prevent*. 2012;49:410–418.
24. Hassan SE, Snyder BD. Street-crossing decision-making: a comparison between patients with age-related macular degeneration and normal vision. *Invest Ophthalmol Vis Sci*. 2012;53:6137–6144.
25. Barrett AM, Houston K. Update on the clinical approach to spatial neglect. *Curr Neurol Neurosci Rep*. 2019;19:25.
26. Barrett AM. Spatial neglect and anosognosia after right brain stroke. *Continuum (Minneap Minn)*. 2021;27:1624–1645.
27. Vossel S, Weiss PH, Eschenbeck P, Saliger J, Karbe H, Fink GR. The neural basis of anosognosia for spatial neglect after stroke. *Stroke*. 2012;43:1954–1956.
28. Heilman KM. Intentional neglect. *Front Biosci (Landmark Ed)*. 2004;9:694–705.
29. Tomasi M, Pundlik S, Bowers AR, Peli E, Luo G. Mobile gaze tracking system for outdoor walking behavioral studies. *J Vis*. 2016;16:27.
30. Kumar A, Pundlik S, Peli E, Luo G. Comparison of visual SLAM and IMU in tracking head movement outdoors. *Behav Res Methods*. 2022;55:2787–2799.
31. Zihl J. Visual scanning behavior in patients with homonymous hemianopia. *Neuropsychologia*. 1995;33:287–303.

Investigative Ophthalmology & Visual Science

32. Tant ML, Cornelissen FW, Kooijman AC, Brouwer WH. Hemianopic visual field defects elicit hemianopic scanning. *Vis Res*. 2002;42:1339–1348.
33. Sahraie A, Cederblad AMH, Kenkel S, Romano JG. Efficacy and predictors of recovery of function after eye movement training in 296 hemianopic patients. *Cortex*. 2020;125:149–160.
34. Pundlik S, Baliutaviciute V, Moharrer M, Bowers AR, Luo G. Home-use evaluation of a wearable collision warning device for individuals with severe vision impairments: a randomized clinical trial. *JAMA Ophthalmol*. 2021;139:998–1005.
35. Pundlik S, Tomasi M, Luo G. Evaluation of a portable collision warning device for patients with peripheral vision loss in an obstacle course. *Invest Ophthalmol Vis Sci*. 2015;57:2571–2579.
36. Bowers AR, Keeney K, Peli E. Community-based trial of a peripheral prismvisual field expansion device for hemianopia. *Arch Ophthalmol*. 2008;126:657–664.
37. Bowers AR, Keeney K, Peli E. Randomized crossover clinical trial of real and sham peripheral prism glasses for hemianopia. *JAMA Ophthalmol*. 2014;132:214–222.
38. Tomasi M, Churchill J, Wiegand JP, et al. Peripheral prisms increase blindside eye and head scanning movements during outdoor walking in hemianopes: preliminary results. *Invest Ophthalmol Vis Sci*. 2013;54:2758.
39. Houston KE, Bowers AR, Fu X, et al. A pilot study of perceptual-motor training for peripheral prisms. *Transl Vis Sci Technol*. 2016;5:9.
40. Schenkenberg T, Bradford DC, Ajax ET. Line bisection and unilateral visual neglect in patients with neurologic impairment. *Neurology*. 1980;30:509–551.
41. Gauthier L, Dehaut F, Joanette Y. The Bells Test: a quantitative and qualitative test for visual neglect. *Int J Clin Neuropsychol*. 1989;11:49–54.
42. Azouvi P, Bartolomeo P, Beis JM, Perennou D. A battery of tests for the quantitative assessment of unilateral neglect. *Restor Neurol Neurosci*. 2006;24:273–285.
43. Pfeiffer E. A short portable mental status questionnaire for the assessment of organic brain deficit in elderly patients. *J Am Geriatr Soc*. 1975;23:433–441.
44. Xu J, Emmermann B, Bowers AR. Auditory reminder cues to promote proactive scanning on approach to intersections in drivers with homonymous hemianopia: driving with hemianopia, IX. *JAMA Ophthalmol*. 2022;140:75–78.
45. Ramulu PY, Maul E, Hochberg C, Chan ES, Ferrucci L, Friedman DS. Real-world assessment of physical activity in glaucoma using an accelerometer. *Ophthalmology*. 2012;119:1159–1166.
46. Bates D, Mächler M, Bolker B, Walker S. Fitting linear mixed-effects models using lme4. *J Stat Softw*. 2015;67:1–48.
47. Brooks ME, Kristensen K, van Benthem KJ, et al. glmmTMB balances speed and flexibility among packages for zero-inflated generalized linear mixed modeling. *R J*. 2017;9:378–400.
48. Lenth RV. emmeans: estimated marginal means, aka least-squares means. R package version 1.7.2. 2022, https://CRAN.R-project.org/package=emmeans. Accessed November 3, 2023.
49. Lüdecke D, Ben-Shachar M, Patil I, Waggoner P, Makowski D. performance: an R package for assessment, comparison and testing of statistical models. *J Open Source Softw*. 2021;6:3139.
50. DHARMa Hartig F.: residual diagnostics for hierarchical (multi-level /mixed) regression models. R package version 0.4.1. 2021, https://CRAN.R-project.org/package=DHARMa. Accessed November 3, 2023.
51. Wickham H. *ggplot2: Elegant Graphics for Data Analysis*. New York, NY: Springer-Verlag; 2016.
52. Kim R, Kim H-J, Kim A, Jang M-H, Kim H, Jeon B. Validation of the conversion between the Mini-Mental State Examination and Montreal Cognitive Assessment in Korean patients with Parkinson's disease. *J Mov Disord*. 2018;11(1):30–34.
53. Xu J, Baliutaviciute V, Swan G, Bowers AR. Driving with hemianopia X: effects of cross traffic on gaze behaviors and pedestrian responses at intersections. *Front Hum Neurosci*. 2022;16:1–12.
54. Savage SW, Zhang L, Swan G, Bowers AR. The effects of age on the contributions of head and eye movements to scanning behavior at intersections. *Transp Res Part F Traffic Psychol Behav*. 2020;73:128–142.
55. Lococo KH, Staplin L. *Visual Scanning Training For Older Drivers: A Literature Review*. Report No. DOT HS 812 514. Washington, DC: National Highway Traffic Safety Administration; 2018.
56. Tom A, Granié M-A. Gender differences in pedestrian rule compliance and visual search at signalized and unsignalized crossroads. *Accident Anal Prevent*. 2011;43:1794–1801.
57. Holland C, Hill R. Gender differences in factors predicting unsafe crossing decisions in adult pedestrians across the lifespan: a simulation study. *Accident Anal Prevent*. 2010;42:1097–1106.

Appendix A: Background About Previous Studies in This Series

The data analyzed in this study were acquired between 2012 and 2014 from patients concurrently enrolled in one of two studies of perceptual motor training for peripheral prism glasses for HH. The first training study (unpublished) allowed enrollment of patients with homonymous field loss either with or without LHSN, and the second study only enrolled those with complete HH and excluded LHSN.[39] Characteristics of each participant whose data are included in this study are given in Table A1. The experimental procedures were identical for the two studies and included outdoor walks without prism glasses at each of four study visits. At three of the visits, participants also completed a walk with prism glasses (not included in analyses for the current study). The perceptual-motor training was aimed at improving performance with the prism glasses and should have had no effect on outdoor walking behaviors without prism glasses. Indeed, preliminary analyses confirmed that visit number was not a significant factor affecting gaze-scanning rates or scan magnitudes.

Appendix B: Generation of Fused Head Movement Signal

Head movements in the outdoor walking data were independently estimated using two methods: SLAM and dual inertial measurement units (IMUs).

SLAM tends to be more accurate than the IMU method in outdoor settings. The IMU signal drifts over time, which can be considered a slow drift over many minutes, and low-pass filtering can help address this issue. However, SLAM suffers from intermittent data loss, whereas the IMU signal is more or less continuous. Thus, there is a trade-off between accuracy and data availability. The

Table A1. Individual Patient Characteristics

Subjnum	Age (y), Bio-Gender	Race	HH	Cause	Duration (y)	Dominant Hand	Clinician Impression of LSN Severity	Bells Test Omissions (R-L)	SLBT Mean % dev.	CBS Trouble Adjusting L Sleeve	CBS Trouble Find Way L	History of LSN	Cognition (MMSE or MoCA)	BCVA (OU, or Better Eye if OU Unavailable)
1	34, M	C	Right, c	Aneurysm, L-F-T	1.4	R	None	0	2.5	N	N	N	29	20/16
2[*]	20, M	C	Left, i	Stroke, ischemic, R-Oc	2.9	R	None	−1	−0.8	N	N	N	29	20/25
3	**81, M**	**AA**	**Left, c**	**Stroke, R-P-Oc**	**4.2**	**R**	**Moderate**	**5**	**−12.0**	**Y**	**Y**	**Y**	**15[†]**	**20/30**
4	83, F	C	Right, c	Stroke, L O-T	1.9	R	None	1	−2.9	N	N	N	28[†]	20/20-1
5	77, F	C	Left, c	Stroke, Ischemic, R-Oc	2.0	R	None	0	−7.7				30	20/30+1
6	**70, M**	**C**	**Left, c**	**Stroke, R-T-Oc**	**0.7**	**R**	**Mild**	**0**	**−8.8**	**N**	**N**	**Y**	**30**	**20/32**
7	46, M	C	Right, c	Abscess, L-P-Oc	12.3	L	None	0	6.1	N	N	N	21	20/20
8	46, M	C	Left, c	Lobectomy, R-T	16.1	L	None	1	−1.8	N	N	N	29	20/20
9	**53, M**	**C**	**Left, c**	**TBI**	**15.7**	**R**	**Moderate**	**−4**	**0.5**	**N**	**N**	**Y**	**26**	
10	63, M	C	Right, c	L-PCA	0.5		None	−2	11.8	N	N	N	24	20/25
11	62, M	C	Left, c	Stroke, embolic, R-P-O	3.2	R	None	1	−5.9	N	N	N	30	20/20
12	**47, M**	**C**	**Left, c**	**Brain tumor**	**23.0**	**R**	**Mild[‡]**	**0**	**−6.1**				**25**	**20/20**
13	47, F	C	Left, c	Aneurysm, R-T	4.1	L	None	−2	−21.0	N	N	N	29	20/30+2
14	**21, M**	**C**	**Left, c**	**Aneurysm**	**1.4**	**L**	**Mild**	**3**	**−9.5**	**Y**	**Y**	**Y**	**27**	**20/25**
15[§]	52, F	C	Left, i	Stroke	0.3	R	None	0	−12.9	N	N	N	29	20/25+2
16[‖]	**36, M**	**C**	**Left, i**	**Aneurysm, L-T-P, ICH**	**2.8**	**R**	**Mild**	**−2**	**−2.1**	**N**	**N**	**Y**	**27**	**20/20**
17	78, M	C	Right, c	Ischemic L-PCA	1.1	R	None	−3	5.4			N	24	20/25
18	61, F	C	Right, c				None	0	−8.8				30	20/20
19	76, M	C	Right, c	Stroke, embolic L-Oc	0.7	R	None	−1	1.7				27	

Bold rows indicate patients with left hemispatial neglect. MMSE and MoCA are out of 30 possible. AA, African American; BCVA, best corrected visual acuity; C, Caucasian; c, complete HH; CBS, Catherine Bergego Scale (neglect symptom scale); dev., deviation (positive values = rightward line bisection error, negative values = leftward line bisection error); F-T, fronto temporal; HH, homonymous hemianopia; i, incomplete HH; ICH, intracerebral hemorrhage; L, left; LSN, left spatial neglect; MoCA, Montreal Cognitive Assessment; N, no; Oc, occipital; P, Pareital; PCA, posterior cerebral artery R, right; SLBT, Schenkenberg line bisection test; T, temporal; TBI, traumatic brain injury; Y, yes.

[*] Central 5° diameter field intact.

[†] Montreal Cognitive Assessment: Converted to MMSE Score[2].

[‡] Subject 12 missed a line on the left of the line bisection test, starts on right slow to scan left on Bells test.

[§] Blind field extends from center to 60° horizontally, and until 50° inferior to center.

[‖] Central 10° radius field intact.

Table B1. Missing SLAM Data and the Characteristics of the Corresponding IMU Data for Three Participants

Participant	No. of Segments With SLAM Data Missing	Segments With Large Horizontal or Vertical Scans	% of Missing SLAM Segments With Large Horizontal or Vertical Scans	Mean IMU Yaw Magnitude (°) When SLAM Data Are Present	Mean IMU Yaw Magnitude (°) When SLAM Data Are Missing
(LHSN)	38	37	97	4.5	11.6
(RHH)	57	44	77	5.6	9.8
(LHH)	58	49	84	7.8	16.5

Average magnitude, as measured by IMU, was significantly larger in segments where SLAM data were missing, indicating the presence of larger head turns during these missing sections. A large percentage of missing SLAM segments involved at least one large horizontal (>20°) or vertical (>10°) head movement, indicating that SLAM missing data were associated with large-magnitude head turns.

data from the two methods, SLAM and IMU, were obtained independently, and then fused based on a straightforward rule-based procedure with the goal of maximizing the availability of valid data.

Our previous work[29,30] demonstrated that (1) SLAM is more accurate than IMU for head movement estimation, and (2) IMU output is relatively more robust for large head turns compared to small head movements. Therefore, whenever available, SLAM estimates were used for small angle head movements. For larger angles, the SLAM signal was retained only if it agreed with the IMU signal. IMU was used whenever SLAM was missing because missing SLAM segments usually involved large head movements (Table B1). Therefore, if IMU output filled in for the missing SLAM data, it was more likely to be for large-magnitude head turns and therefore likely to be robust.

Steps to fuse IMU and SLAM head movement data:

1. Convert SLAM quaternion values to Euler angles: yaw, pitch, and roll.
2. Find missing data in SLAM, and obtain the index of available data segments (for yaw and pitch).
3. Separately for yaw and pitch from both methods, for each available data segment:
   a. Find the moving median signal (window size 450 frames).
   b. Detrend by subtracting the moving median from the original signal.
   c. Determine the relative shift between signals of both methods via cross-correlation (window size: 30 frames).
   d. Shift the IMU signal to align with SLAM signals—separately for yaw and pitch (IMU tends to be misaligned with respect to video).
4. For a moving window (30 frames), find the local cross-correlation coefficient between SLAM and IMU separately for yaw and pitch.
5. Find disagreements between two methods where correlation coefficient is low (<0.5), and ignore disagreements for small magnitudes (<10°).
6. Merging the signals; at each sample:
   a. If good agreement (correlation coefficient ≥0.5), use SLAM.
   b. If SLAM missing, use IMU.
   c. If abnormal IMU (magnitude over 90°), set to not a number (NaN).
   d. If both disagree (correlation coefficient <0.5), set to NaN.

Appendix C: Detection of Gaze Scans

Gaze scans were detected based on a significant deviation of the gaze position on either side of the straight-ahead direction or the mean heading direction (magnitude threshold 20°) for at least a minimum threshold duration of time (135 ms). There were two kinds of gaze scans: larger-magnitude scans driven by head movement (Fig. C1A) and smaller-magnitude scans driven by eye movement (Fig. C1B). As the name suggests, head movement was a large component of the head movement–driven scans, with concordant eye movements typically adding to the head position to determine the gaze position. For detection of head movement–driven gaze scans, a minimum threshold of 10° and 20° was used for the head movement and the overall gaze movement, respectively. The head and gaze peaks usually did not align, and sometimes the eye movement signal was lost at the peak head position. Therefore, the gaze peak position for the head-driven gaze scan was determined as the maximum gaze magnitude located within the time window defined by the ± two-thirds of peak head position on either side of the head position peak (Fig. C1A). In addition to head-driven gaze scans, eye movement–driven gaze scans were detected when gaze magnitude exceeded 20° for a minimum duration of 135 ms. The two kinds of gaze scans were merged; repeated eye movement–driven gaze scans detected within ±430 ms of a peak head scan were merged with the corresponding head-driven gaze scan. Head movement–driven gaze scans tended to be larger in magnitude and longer

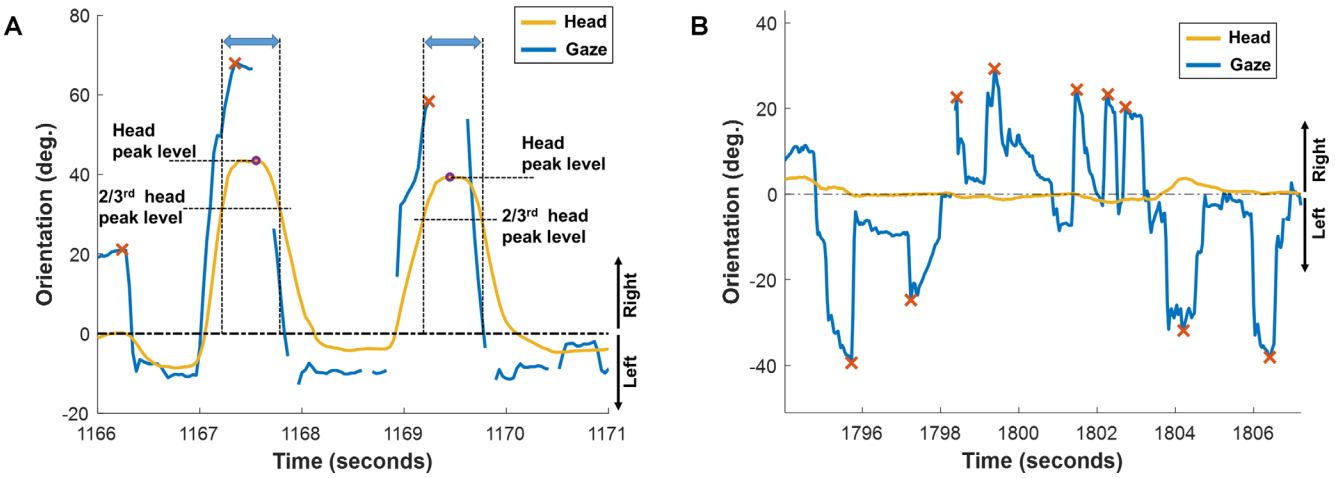

Figure C1. Detection of horizontal gaze scans (negative orientation values indicate scans toward the left side). (**A**) Head movement–driven gaze scans. Gaze can be discontinuous due to intermittent loss of eye tracking. The peak gaze scans (shown by *red x*) are the maximum gaze signal within ± two-thirds of the head movement peak signal (shown by a *purple open circle*). The duration span of ± two-thirds of peak head positions for each of two scans is shown by *horizontal blue double headed arrows*. (**B**) Eye movement–driven gaze scans. The gaze scans (*blue line*; scan peak shown by *red x*) are all due to large eye movements. The head movement (*orange line*) is minimal in this sequence.

in duration (of the order of many hundred milliseconds) compared to the eye movement–driven gaze scans.

Appendix D: Statistical Analysis Details

R Packages Used

Linear mixed-effects regression (for gaze magnitude as the outcome) was carried out using the R package "lme4."[46]

Computation of estimated marginal means was done using R package "emmeans."[48]

Mixed-effects negative binomial count regression (for scan rate) was carried out using the R package "glmmTMB."[47]

Model diagnostics were performed using the "performance" package[49] and with the "DHARMa" package for the negative binomial model.[50]

Linear Regression Model for Gaze Scan Magnitude

The outcome variable was gaze magnitude, which was transformed as the reciprocal inverse of its logarithm (denoted by gazemag).

The predictors (fixed) were scanside (whether the scan was toward the BlindSide or the SeeingSide), group (subject group LHH, LHSN, or RHH), crphase (crossing phase: approach or crossing), and cwtype (crossing type—signalized or nonsignalized crossings).

Study visit (1 through 4, denoted by visit) was nested within the subject factor (denoted by subjnum) as random intercepts. Interactions between group, scanside, and crphase, as well as between group and cwtype factors, were included.

The model was specified as follows:

$$gazemag \sim scanside + group + crphase + cwtype + scanside{:}crphase + group{:}scanside + group{:}crphase + group{:}scanside{:}crphase + group{:}cwtype + (1|subjnum/visit)$$

Model evaluation was performed in the following ways:

1. checking model diagnostics—plots and with parametric testing,
2. comparison with a null model, and
3. visual comparison of the data simulated from the fitted model with the observed data.

Figure D1 shows the model diagnostic plots—fitted values versus residuals—to check the linearity assumption (top left), homogeneity of variance (top right), QQ plot for checking the normality of residuals (bottom left), and density of the distribution of the residuals (bottom right). In the top-left plot in Figure D1, the reference line (green line) in the plot is close to the horizontal line. Similarly, the assumption regarding the homogeneity of variance also seems to be met based on Figure D1 (top right) and from parametric testing (Bartlett's test statistic = 20.4, $df = 23$, $P = 0.62$). The typical S-shaped curve in the QQ plot indicates that the residuals seem to deviate slightly from normality. However, given the large number of observations (>5000), deviation from normality may not be a serious violation. Comparison for model Akaike informa-

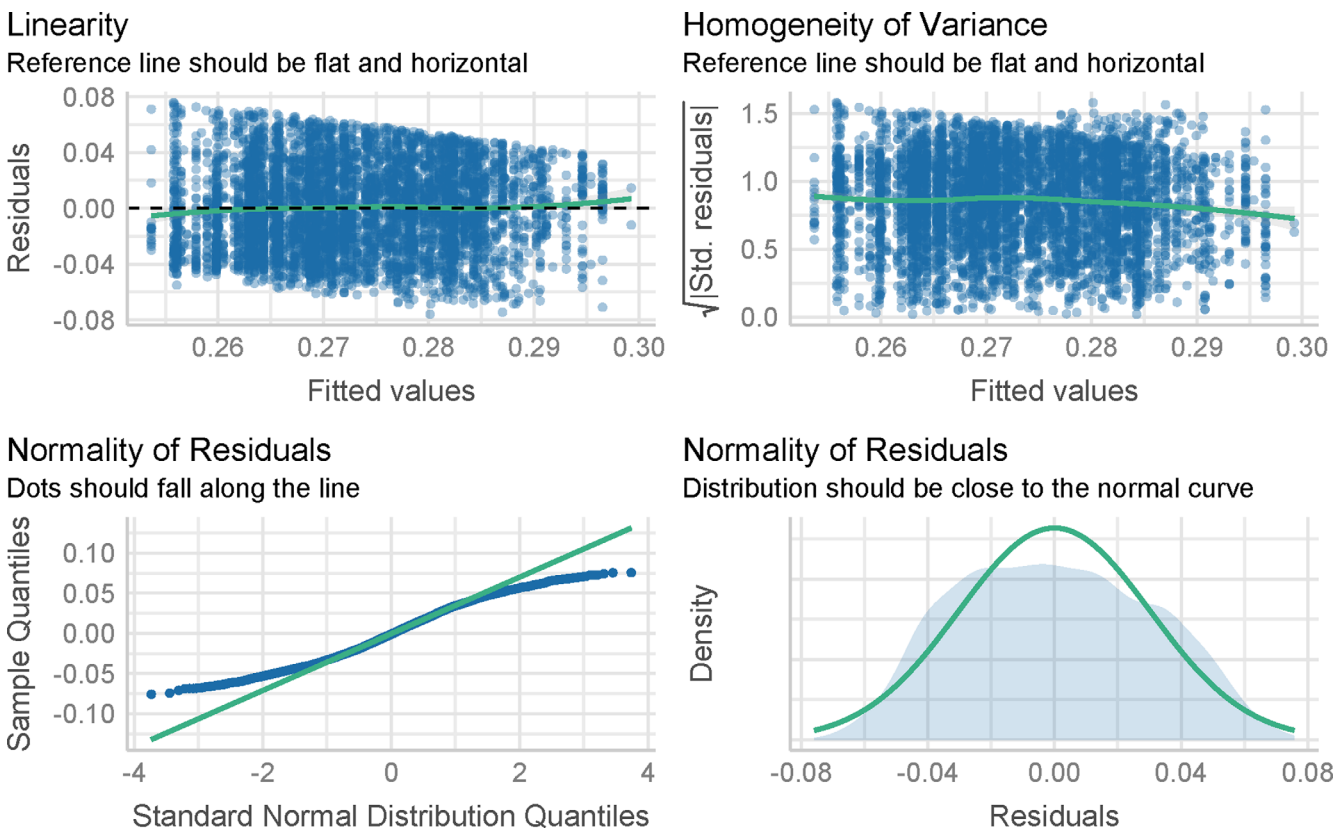

Figure D1. Diagnostic plots from the regression model for gaze magnitude. In the scatterplots in the *top row*, the reference line (*green line*) in the plot is close to the horizontal line, indicating that linearity and homogeneity assumptions are not violated. The *bottom row* shows plots indicating normality of residuals, where there seems to be slight deviation from normality. However, given the very large number of observations, this violation may not be serious.

Table D1. Comparison of Akaike Information Criterion (AIC) Values for Various Models Versus the Fitted Model for Gaze Magnitude

Name	AIC	AIC Weights
Null model (intercept only)	−21,964	<0.001
Fixed effects (FE) only	−22,106	<0.001
Subject as random intercept (no nested visit)	−22,184	<0.001
Visit as a FE (subject as random intercept)	−22,185	<0.001
No interactions between the FEs	−22,166	<0.001
Remove scanside factor	−22,058	<0.001
Remove group factor	−22,161	<0.001
Remove crossing phase factor	−22,083	<0.001
Remove crossing type factor	−22,200	0.045
Full model (fitted model)	−22,206	0.955

The fitted model as specified above (for which the results were presented) has the lowest AIC value compared to the others.

tion criterion (AIC) values (Table D1) shows that the model specified above was the best compared to the null model or model with just fixed effects or models after dropping various key predictors and their respective interaction terms. Finally, data simulated from the fitted model were consistent with the observed data (Fig. D2), indicating a valid model fit.

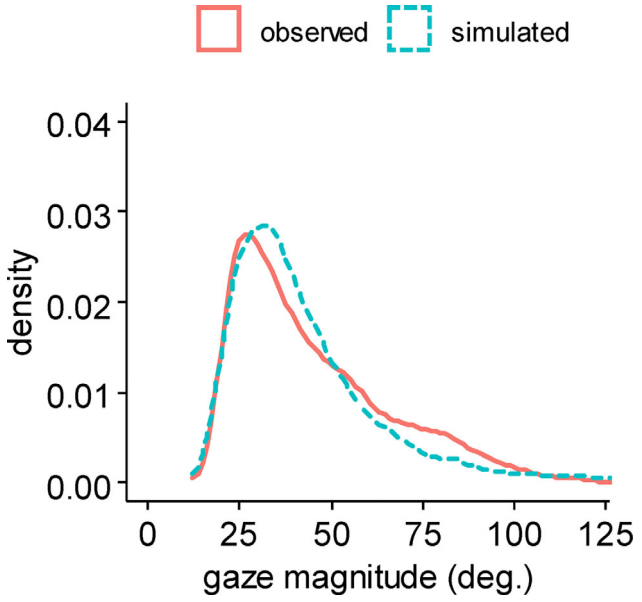

Figure D2. Gaze magnitude density comparison between observed data and data simulated from the fitted model. Broadly, the simulated data distribution is consistent with the observed data, indicating a valid model fit. It should be noted that observed and simulated gaze magnitudes are skewed toward the lower values.

Investigative Ophthalmology & Visual Science

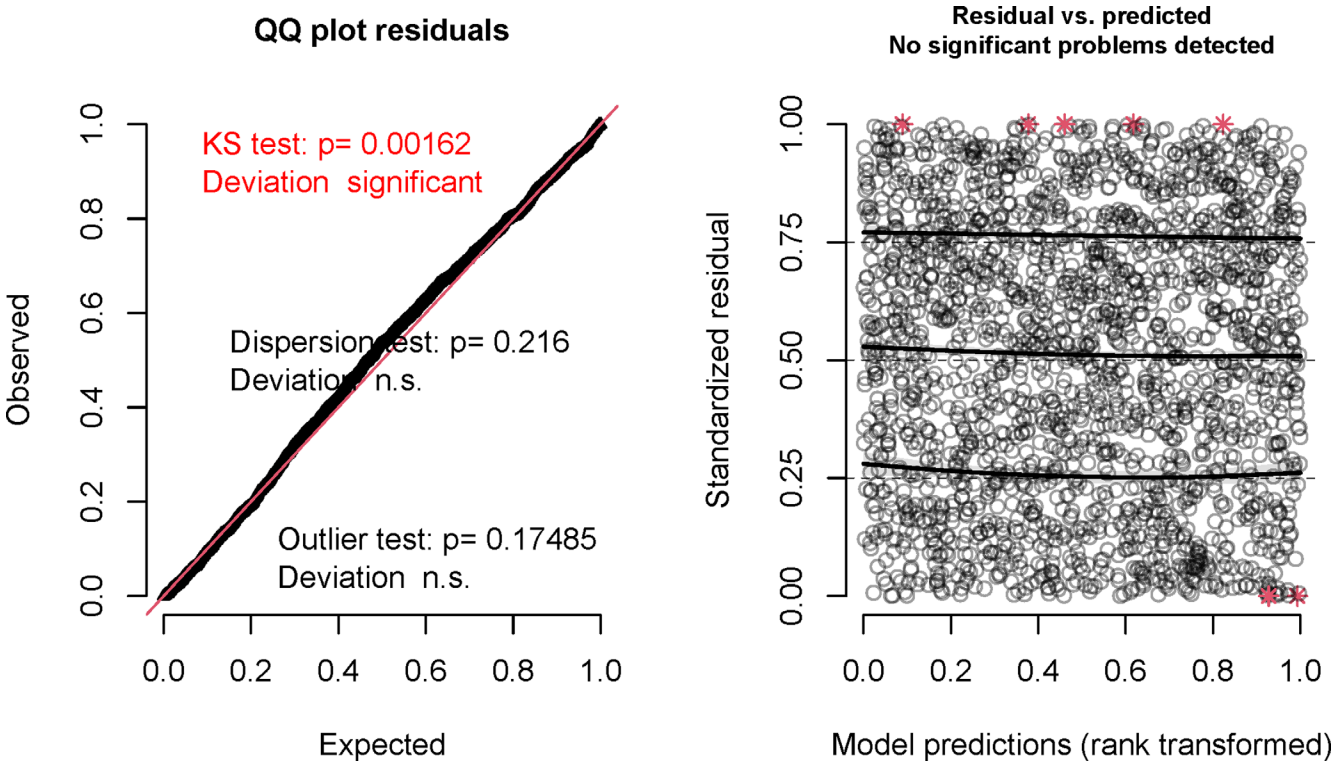

Figure D3. Diagnostic plots for scanning rate regression model: (*left*) QQ plot and (*right*) scatterplot of the residuals. The *horizontal lines* in the scatterplot to the *right* are the quantile regression lines. Since they are close to flat, this is an indication that the residuals are uniformly distributed and there are no major issues in model specification. QQ, quantile-qunatile.

Negative Binomial Model for Scanning Rate

Scanning rate was modeled as number of scans (denoted by nscans) as the dependent variable in a count regression model, with the log of time duration (duration) included as the offset. The predictors (fixed) were age (subject age in years), scanside (whether the scan was toward the BlindSide or the SeeingSide), group (subject group LHH, LHSN, or RHH), crphase (crossing phase: approach or crossing), and cwtype (crossing type—signalized or nonsignalized crossings). Study visit (1 through

Table D2. Comparison of AIC Values for Various Models Versus the Fitted Model for Scanning Rate

Name	AIC	AIC Weights
Null model	6,871.911	<0.001
Fixed effects (FE) only	6,915.632	<0.001
Subject as random intercept (no nested visit)	6,835.532	<0.001
Subject as random intercept, visit FE	6,816.363	<0.001
No interactions	6,771.737	0.035
Remove age variable	6,773.764	0.013
Remove scanside factor	6,791.705	<0.001
Remove group factor	6,766.869	0.394
Remove crphase factor	6,844.739	<0.001
Remove cwtype factor	6,769.759	0.093
Full model as specified	6,766.530	0.466

The model for which the results were presented has the lowest AIC value compared to the others.

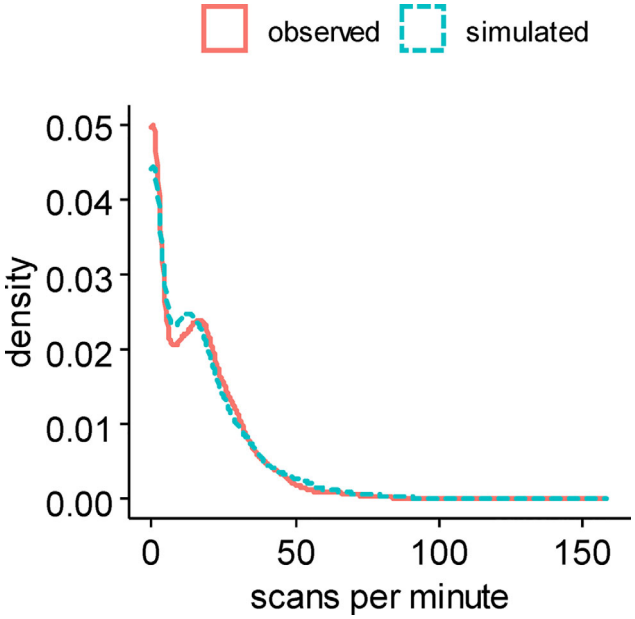

Figure D4. Scan rate (scans per minute) density comparison between observed data and data simulated from the fitted model. Broadly, the simulated data distribution is consistent with the observed data, indicating a valid model fit.

4, denoted by visit) was nested within the subject factor (denoted by subjnum) as random intercepts. Interaction between crphase and cwtype factors was included. The model was specified as follows:

$$nscans \sim age + scanside + group + crphase * cwtype + offset * \left(log\left(duration\right)\right) + \left(1|subjnum/visit\right)$$

Similar to the gaze magnitude analysis above, scanning rate model evaluation was performed in the following ways:

1. checking model diagnostics—plots and with parametric testing,
2. comparison with a null model, and
3. visual comparison of the data simulated from the fitted model with the observed data.

Figure D3 shows the model diagnostic plots—the QQ plot of the residuals (left) and the residuals scatterplot (right). Statistically significant kolmogorov smirnov (KS) test indicates deviation of the residuals from uniformity, perhaps due to the large number of observations that make it highly sensitive to even slight deviation from uniformity. The scatterplot is overlaid with quantile regression lines at 0.25, 0.5, and 0.75 quantiles, which are mostly flat. This indicates that the residuals are mostly uniformly distributed and the model is likely to be correctly specified. The dispersion test was not significant (Pearson χ^2 dispersion = 0.93, df = 2073, P = 0.99). Also, the zero-inflation test was not significant (ratio = 0.98, P = 0.64). Comparison of the model as specified versus the null model and the various other forms is shown in Table D2. The model as specified had the lowest AIC value compared to other variations. Finally, Figure D4 shows the comparison between the observed data and the data simulated with the fitted model. The density curves appear very similar, indicating that the fitted model may be valid.